Electronic Supplementary Material (ESI) for Journal of Materials Chemistry A.

Supporting information

In situ synthesis of highly active $Na_2Ti_3O_7$ nanosheet on activated carbon fiber as anode for high-energy density supercapacitors

Xiaoming Qiu[a], Xuan Zhang[b], Li-Zhen Fan[a]*

[a] Beijing Advanced Innovation Center for Materials Genome Engineering, Institute of Advanced Materials and Technology, University of Science and Technology Beijing, Beijing 100083, China

[b] Department of Biochemistry, University of Wisconsin-Madison, WI,53705, United States

*Corresponding author: E-mail: fanlizhen@ustb.edu.cn

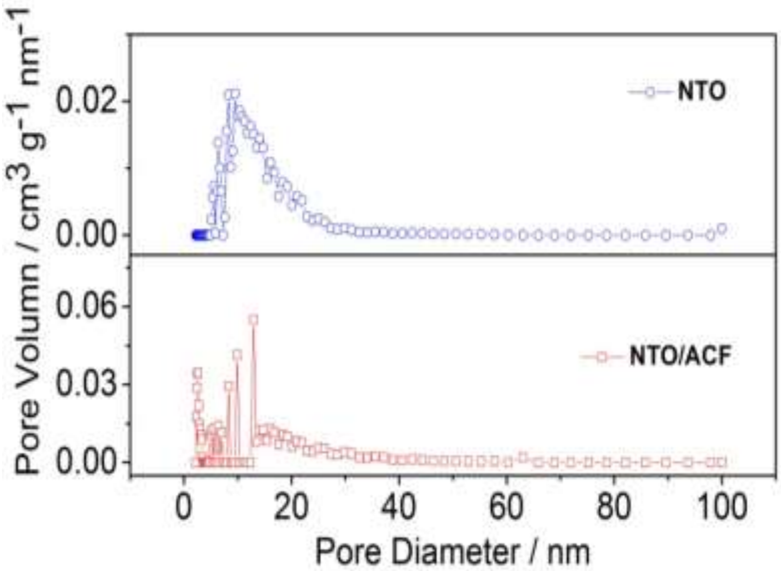

Fig. S1 The pore size distribution curves

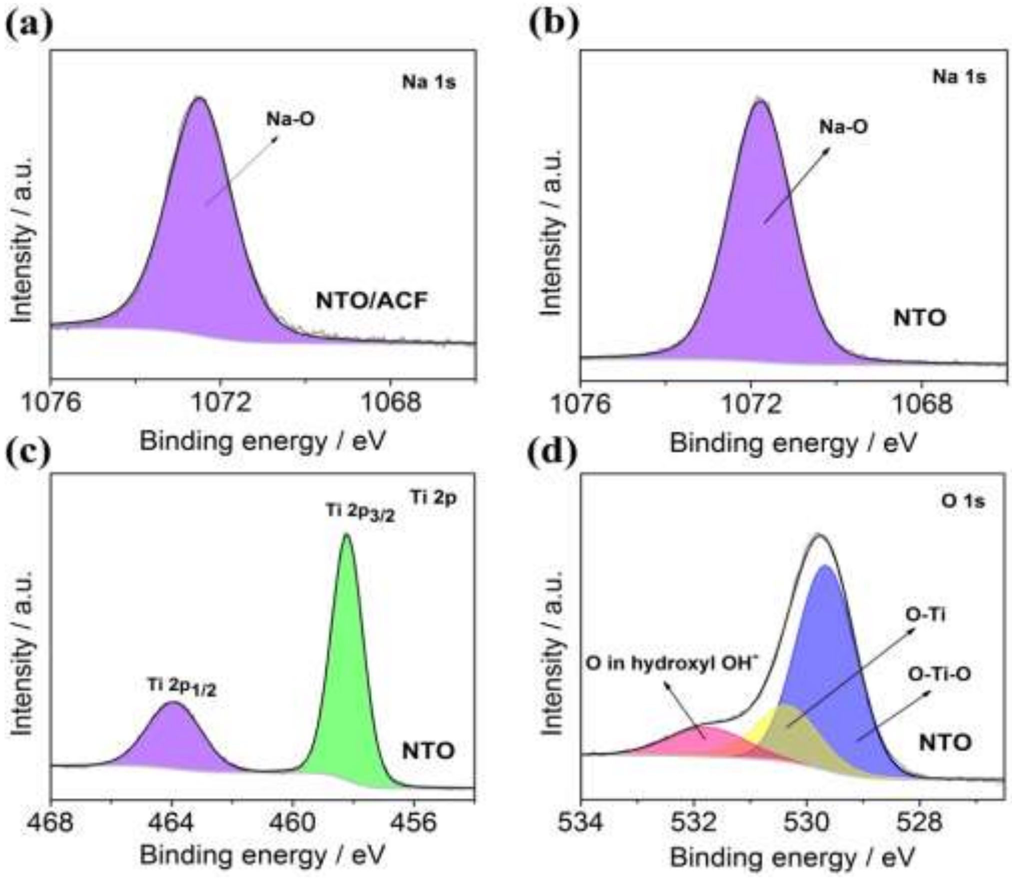

Fig. S2 (a) high resolution XPS spectra of Na 1s, high resolution XPS spectra of (b) Ti 2p, (c) Ti 2p, and (d) O 1s for NTO.

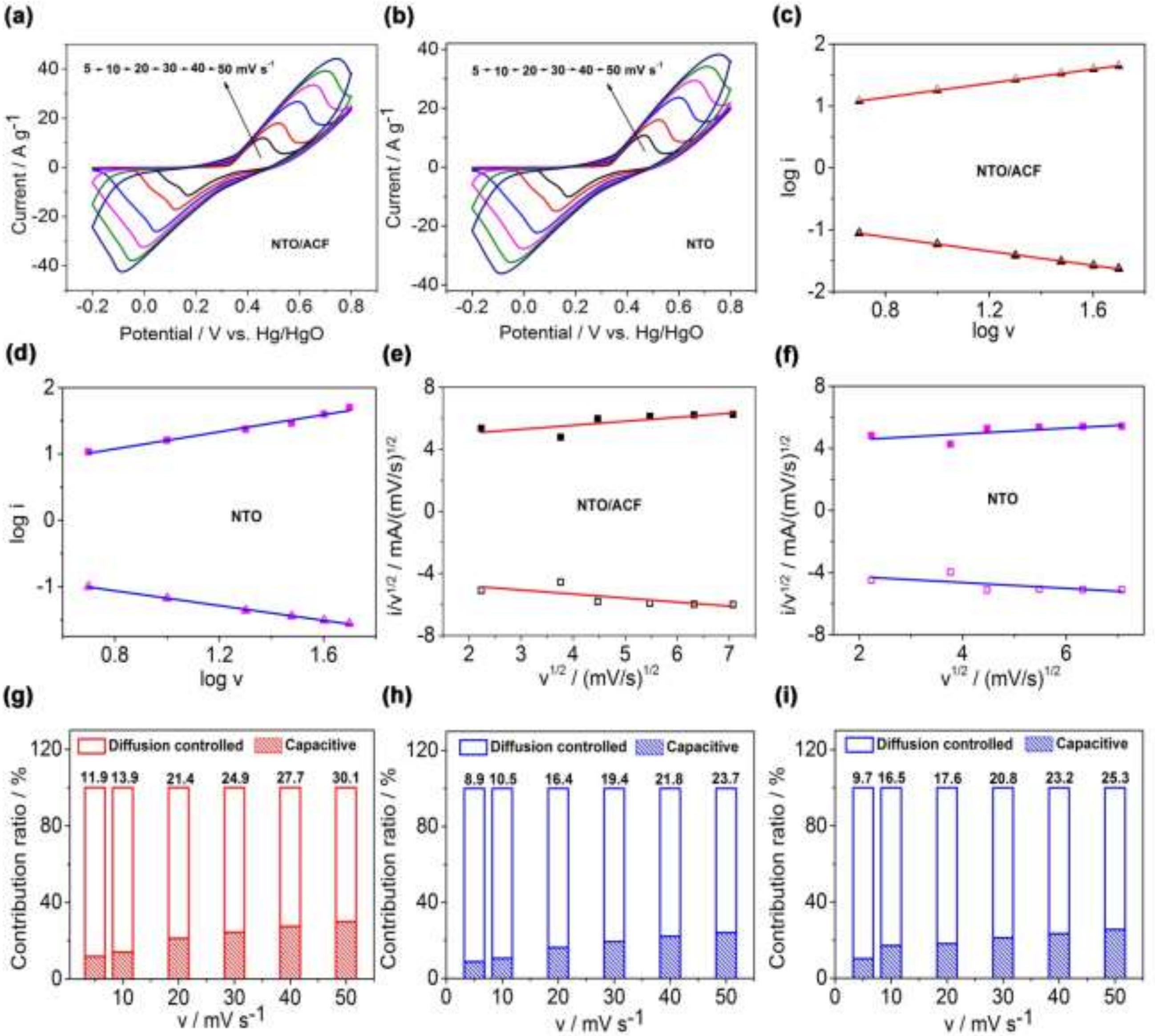

Fig. S3 CV curves of (a) NTO/ACF and (b) NTO at different scan rates. The dependence of parameter b on (c) NTO/ACF and (d) NTO. The plot of the current at different scan rates for (e) NTO/ACF and (f) NTO. The column graphs of contribution ratio of the intercalated and capacitive charge versus scan rate for (g) NTO/ACF nanocomposite under anodic scanning, (h) NTO under cathodic scanning, and (i) NTO under anodic scanning.

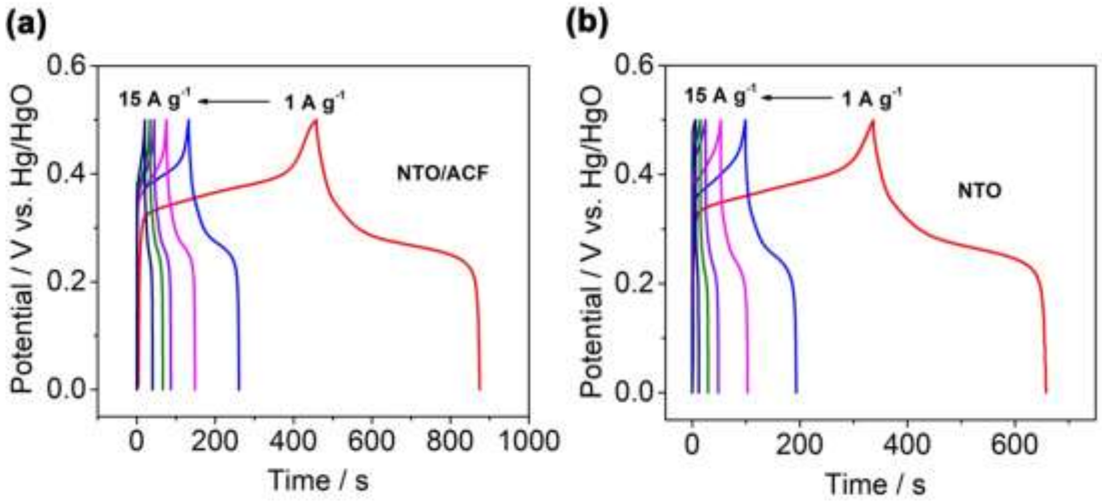

Fig. S4 galvanostatic charge-discharge curves at different current densities of NTO/ACF nanocomposite (a) and pure NTO (b) in 1 mol L^{-1} KOH solution.

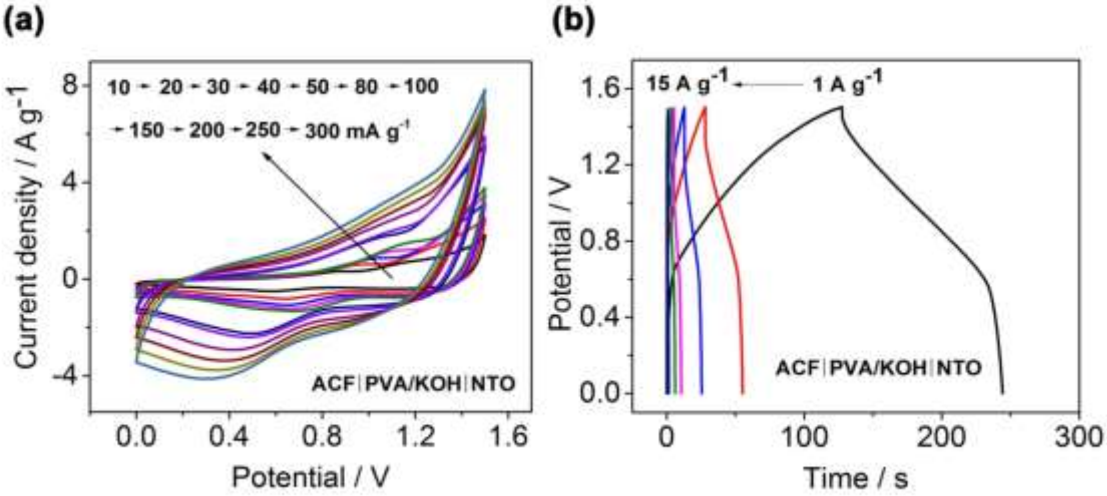

Fig. S5 (a) CV curves at different scan rates, and (b) Charge–discharge curves at different current densities of the ACF//NTO in a PVA/KOH gel electrolyte.

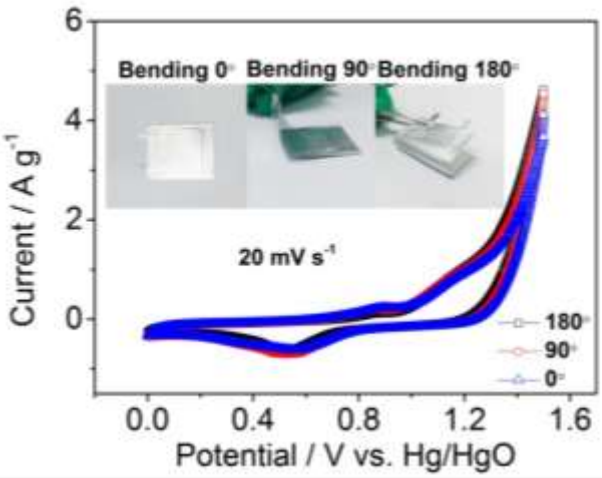

Fig. S6 CV curves of the ACF//NTO/ACF in a PVA/KOH gel electrolyte at a scan rate of 20 mV s^{-1} at different bending angles.

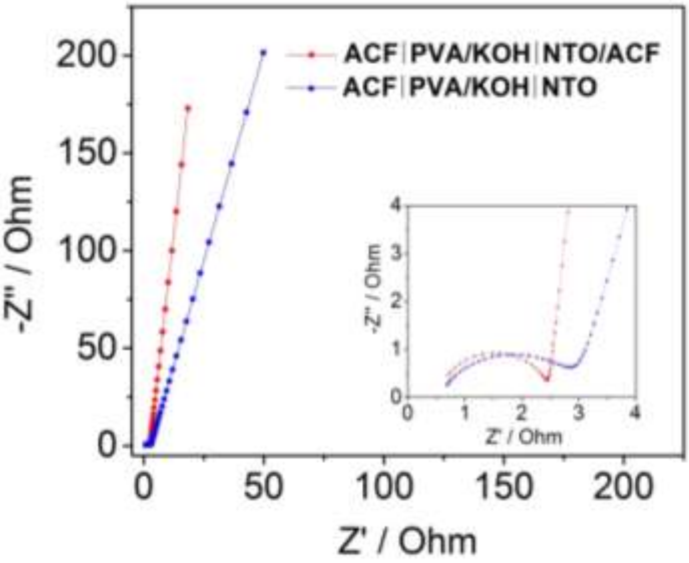

Fig. S7 Nyquist plots of the asymmetric supercapacitors in a PVA/KOH gel electrolyte (the inset shows the magnified high frequency range).

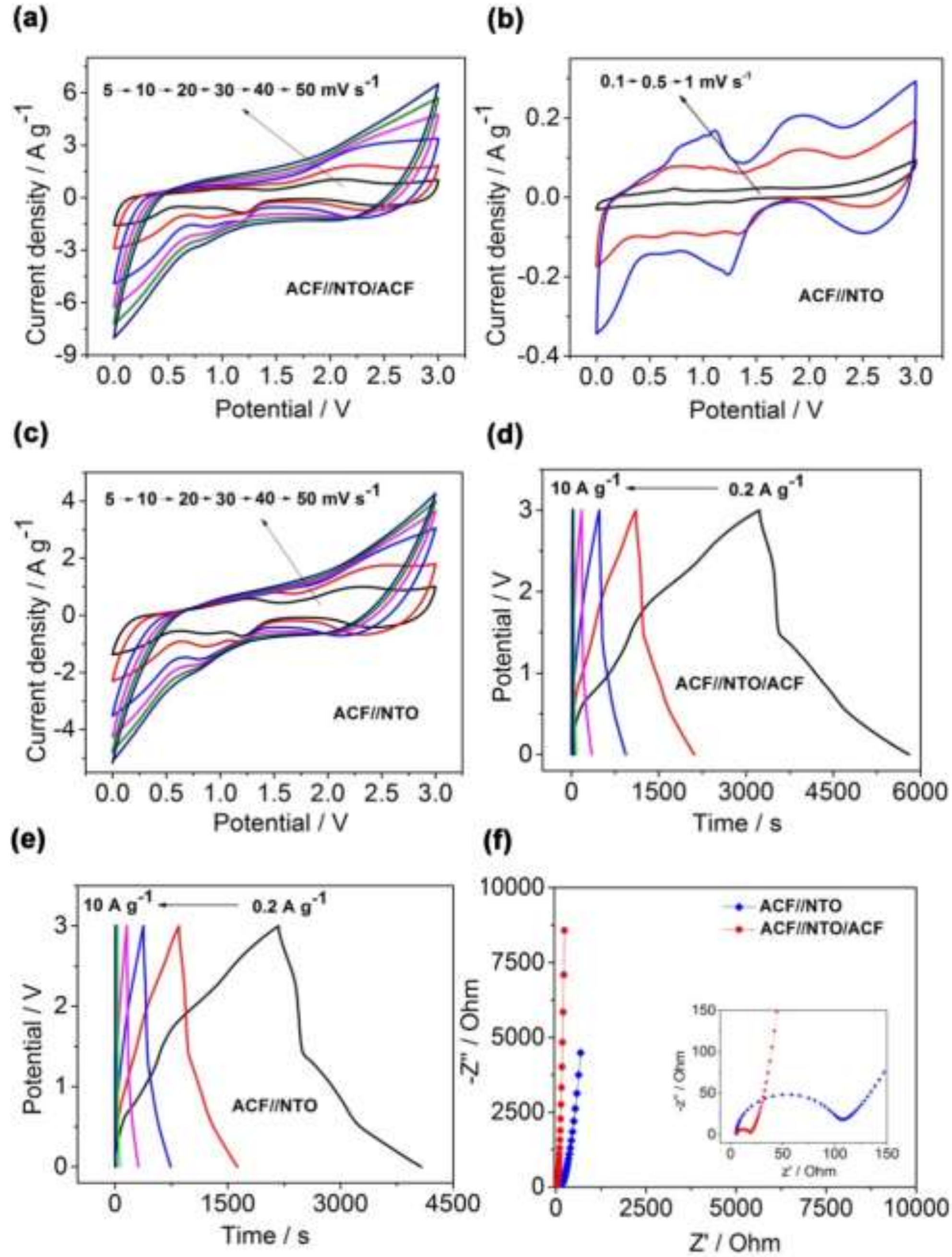

Fig. S8 Electrochemical performance of sodium ion hybrid capacitor measured in 1 mol L^{-1} $NaClO_4$ in propylene carbonate (PC)/fluoroethylene carbonate (FEC) (10: 1 v/v). (a) CV curves of the ACF//NTO/ACF at current densities from 5 to 50 mV s^{-1}, (b) CV curves of the ACF//NTO at current densities of 0.1, 0.5, and 1 mV s^{-1}, (c) CV curves of the ACF//NTO at current densities from 5 to 50 mV s^{-1}, Charge–discharge curves at different current densities of (d) ACF//NTO/ACF and (e) ACF//NTO, and (f) Nyquist plots of the sodium ion hybrid capacitor (the inset shows the magnified highfrequency range).

Table S1 Pore structure parameters of the samples calculated from nitrogen adsorption/desorption isotherms.

Sample	S_{BET} (m^2 g^{-1})[a]	S_{micro} (m^2 g^{-1})[a]	$S_{meso+macro}$ (m^2 g^{-1})[a]	V_{total} (cm^3 g^{-1})[b]	V_{micro} (cm^3 g^{-1})[b]	$V_{meso+macro}$ (cm^3 g^{-1})[b]	APS (nm)[c]
NTO	48	4	44	0.21	0.002	0.208	16.9
NTO/ACF	288	55	233	0.36	0.024	0.336	5.05

a Multipoint Brumauer-Emmett-Teller (BET) method and V-t plots, respectively, and the surface area of the meso/macropores ($S_{meso+macro}$) was acquired by subtracting S_{micro} from S_{total}.

b Total pore volumes (V_{total}) were calculated from the amount adsorbed at a relative pressure P/P_0 of 0.997. Micropore volumes (V_{micro}) were calculated using the t-plot method. The algorithm of meso/macropore ($V_{meso+micro}$) was similar to that of $S_{meso+macro}$.

c Average pore size (APS). Micropore size distributions were determined from the adsorption branches of the isotherms based on the density functional theory (DFT).

Table S2 The equations based on CV curves for NTO/ACF and NTO

Cathodic	$\log(i)=b\log(v)+\log a$	b	$i/v^{1/2}=k_1v^{1/2}+k_2$
NTO/ACF	$\log(i)=0.5648\log(v)+0.68338$	0.56848	$i/v^{1/2}=0.25732\,v^{1/2}+4.51627$
NTO	$\log(i)=0.64338\log(v)+0.56264$	0.64338	$i/v^{1/2}=0.18441\,v^{1/2}+4.18899$
Anodic	$-\log(i)=b\log(v)+\log a$	b	$-i/v^{1/2=}k_1v^{1/2}+k_2$
NTO/ACF	$-\log(i)=-0.57449\log(v)-0.65869$	5.57449	$-i/v^{1/2}=-0.2602\,v^{1/2}-4.28625$
NTO	$-\log(i)=-0.55933\log(v)-0.61564$	0.55933	$-i/v^{1/2}=-0.18651\,v^{1/2}-3.89551$

Table S3 Comparison of specific capacitance of carbon fibers composites and titanate composites

Materials	Current density	Capacitance	Electrolyte	Reference
Hollow carbon microfibers	0.5 A g^{-1}	304.65 F g^{-1}	6 M KOH	1
CF(Ⅲ)	0.3 A g^{-1}	221.7 F g^{-1}	3 M KOH	2
CNF/graphene	1 A g^{-1}	183 F g^{-1}	6 M KOH	3
ZnO/ACF	1 mA cm^2	178.2 F g^{-1}	6 M KOH	4
Li_2TiO_3	1 A g^{-1}	195 F g^{-1}	3 M KOH	5
$Na_2Ti_2O_4(OH)_2$	5 mV s^{-1}	300 F g^{-1}	1 M KOH	6
$C/Na_2Ti_5O_{11}$	1 A g^{-1}	533 F g^{-1}	3M NaOH	7
NTO/ACF	1 A g^{-1}	945.8 F g^{-1}	1 M KOH	This work

References

1 H. Tan, X. Wang, D. Jia, P. Hao, Y. Sang and H. Liu, *J. Mater. Chem. A*, 2017, **5**, 2580-2591.

2 Y. Liu, Z. Shi, Y. Gao, W. An, Z. Cao and J. Liu, *ACS Appl. Mater. Inter.*, 2016, **8**, 28283-28290.

3 Q. Dong, G. Wang, H. Hu, J. Yang, B. Qian, Z. Ling and J. Qiu, *J. Power Sources*, 2013, **243**, 350-353.

4 C. H. Kim and B. Kim, *J. Power Sources*, 2015, **274**, 512-520.

5 H. Mao and B. Li, *Nano*, 2018, **13**, 1850027.

6 R. A. Aziz, I. I. Misnon, K. F. Chong, M. M. Yusoff and R. Jose, *Electrochim. Acta*, 2013, **113**, 141-148.

7 C. Zhang, Y. Xi, C. Wang, C. Hu, Z. Liu, M. S. Javed, M. Wang, M. Lai, Q. Yang and D. Zhang, *J. Mater. Sci*, 2017, **52**, 13897-13908.